Indian Journal of Chemical Technology
Vol. 32, November 2025, pp. 800-811
DOI: 10.56042/ijct.v32i6.14542

Unlocking the potential: Bacterial exopolysaccharide as a smart drug-delivery vehicle for controlled *in vitro* drug release

Sivasankari Marimuthu*, Praveena M, Sakthi Aishvaryaa C & Saranya S

Department of Biotechnology, Mepco Schlenk Engineering College (Autonomous), Sivakasi, Tamil Nadu, India

*E-mail: sivasankari@mepcoeng.ac.in

Received 22 October 2024; accepted 3 November 2025

Conventional methods of drug administration often face limitations such as poor bioavailability, rapid clearance, and undesirable side effects. To overcome these, microbial exopolysaccharides (EPS) have emerged as promising biomaterials due to their ability to serve as biocompatible, biodegradable, and efficient drug carriers. This study focuses on the potential of an EPS extracted from *Bacillus* sp. EPS003 to function as a novel carrier system. Quercetin, a bioactive flavonoid with therapeutic significance, is chosen as the model drug to develop EPS-based quercetin-loaded microparticles (MPs). The MPs have been structurally characterized using UV-visible and FTIR spectroscopy, while particle size and zeta potential measurements confirmed their uniformity and stability. Thermal properties are analyzed by thermogravimetric analysis and surface morphology with elemental composition is examined through SEM-EDAX. Drug loading efficiency and capacity are quantified, and in vitro release kinetics is studied. The results revealed that quercetin release followed a zero-order kinetic model with a high R^2 value, suggesting diffusion-controlled release. The biofunctional properties of the MPs are also assessed. Antioxidant potential is determined using the DPPH radical scavenging assay, while the anti-inflammatory property is evaluated via egg albumin denaturation. Notably, the quercetin-loaded EPS demonstrated 94.6% anti-inflammatory activity, with enhanced antioxidant and anti-inflammatory effects compared to quercetin or EPS alone. Overall, the findings indicate that EPS from *Bacillus* sp. EPS003 can serve as an excellent drug-delivery vehicle, ensuring controlled release without compromising drug stability or activity, thus offering a novel strategy for therapeutic applications.

Keywords: Drug-delivery vehicle, Exopolysaccharide, *In vitro* drug release, Quercetin

Introduction

Drug molecules can be stored in appropriate forms, such as tablets or solutions for administration, using technical systems called drug-delivery systems. Conventional methods of administering drugs have a number of issues and challenges, such as efficient targeting and full dose absorption, the generation of undesirable secondary effects, and the promotion of damage to organs as well as tissues such as the kidney and liver through inflammation and immune responses. Thus, there is a need for drug-delivery carriers to overcome such challenges by promoting drug adsorption, enhancing drug targeting, avoiding or decreasing secondary effects, and possessing the ability to camouflage drugs from immune cells and proteins. They can influence pharmacological activity by modulating drug release from their carrier, thereby prolonging the delivery of the drug over a longer period of time through controlled release while maintaining drug concentration in the blood within therapeutic limits. Their ability to improve the selectivity, effectiveness, systemic circulation, drug solubility, and safety of drug circulation maximizes therapeutic efficacy and minimizes off-target accumulation in the body. The specificity of the carrier can be enhanced by attaching it to certain ligands and molecules that can actively bind to the surface of the target tissues. This approach is known as active targeting. These delivery systems can also reach target cells through the control of one or more physical or chemical properties, such as pH, temperature, ultrasound, magnetic field, and electric field[1]. The use of drug-delivery carriers has increased due to their biocompatibility, biodegradability, mechanical capabilities, and large surface area.

The technical advantages of drug carriers include high stability, high drug holding capacity, the feasibility of adapting several routes for administration, and the capacity to be used with hydrophilic and hydrophobic molecules[2]. These factors make drug-delivery systems as important as the drug itself. A significant progress has been made by researchers towards the successful development of drug-delivery systems based on organic, inorganic,

and hybrid nanoparticles as drug-delivery carriers for active targeting, especially in chemotherapy[3]. The latest drug-delivery systems are formulated with improved properties, such as small particle size, increased solubility, increased efficacy, specific site targeting, reduced toxicity, and sustained delivery, which have significantly improved the performance of therapeutic agents over conventional dosage forms. An innovative drug carrier can be a micro- or nanostructure such as micelles, nanoparticles, emulsions, or nanofibers. Based on their shape, geometry, and production methods, drug carriers are classified into different types, such as dendrimers, hydrogels, and liposomes. Different polymers, such as lactic acid derivatives, polydopamine, and polysaccharides, have also been used as drug-delivery carriers. Among polysaccharides, microbial or bacterial EPS have gained attention due to their wide range of applications in various fields, such as pharmaceuticals, cosmetics, and the food industry. They are highly biocompatible and versatile, making them suitable for drug-delivery applications. In this current study, exopolysaccharide extracted from a novel soil isolate, *Bacillus* sp. EPS003 was used to load the model drug quercetin. The characteristics of the drug-loaded EPS were studied and reported.

Experimental Section

Bacterial strain and identification

The bacterial strain used in this study, *Bacillus* sp. EPS003, was originally isolated from an agricultural soil sample and characterized in an earlier work[4]. Phylogenetic analysis of the 16S rRNA gene sequence confirmed its close relationship to *Bacillus subtilis* (GenBank accession number OM967419).

EPS production

Overnight culture of *Bacillus* sp. EPS003 was inoculated in 750 mL of EPM (EPS production medium) containing sucrose (10 g L^{-1}), peptone (5 g L^{-1}), yeast extract (2.5 g L^{-1}), dipotassium phosphate (2 g L^{-1}), trisodium citrate (2 g L^{-1}), $MgSO_4.7H_2O$ (0.5 g L^{-1}), $MnSO_4$ (0.05 g L^{-1}), and agar (20 g L^{-1}) and kept at 37°C for 72 h at 160 rpm[5].

EPS extraction and purification

Extraction of EPS was performed by the ethanol precipitation method. The fermented bacterial broth was centrifuged at 7100 rpm for 20 min at 4°C to remove the pellet containing the bacterial cells. Two volumes of prechilled ethanol were added to the supernatant containing the bacterial exopolysaccharide, and the mixture was incubated overnight at 4°C. After incubation, the mixture was centrifuged at 7100 rpm for 20 min at 4°C to separate the pellet containing EPS. The pellet was resuspended in trichloroacetic acid (4% v/v) and incubated at 4°C for 1 h to denature the proteins. The mixture was then centrifuged twice at 7500 rpm for 20 min at 4°C to facilitate the removal of the protein precipitate. The pellet containing the EPS was lyophilized for further use. The chemical composition and purity of the EPS (total carbohydrate: 0.848 ± 0.011 mg/mL; protein: 0.040 ± 0.004 mg/mL) have been previously reported[4].

Preparation of quercetin-loaded EPS

Quercetin-loaded EPS was formulated by a modified precipitation technique. 2 mg of quercetin was dissolved in 5 mL of cell culture-grade methanol before being added to 50 mL of deionized water containing 10 mg of EPS and 0.1 mL of glutaraldehyde. The solution was stirred on a magnetic stirrer at room temperature. The sample was then centrifuged at 6000 rpm for 30 min to obtain a pellet, which was subsequently washed three times with deionized water. Finally, the pellet was freeze dried and used for characterization.

Characterization of quercetin-loaded EPS

Spectral characterization

UV-visible spectra of quercetin, EPS, and quercetin-loaded EPS microparticles were recorded using a UV-visible spectrophotometer (Shimadzu, Japan) in the range of 200 to 500 nm. Further, the important functional groups and integrity of quercetin and EPS in the quercetin-loaded EPS preparation were analyzed using Fourier transform infrared spectroscopy (FTIR). The FTIR spectrum was obtained in the spectral range of 4000 to 500 cm^{-1} with 4 cm^{-1} resolution following the KBr pellet method using an IR Tracer-100 FTIR spectrophotometer (Shimadzu, Japan).

Particle size and zeta potential

The average particle size and zeta potential of quercetin-loaded EPS formulations were determined following the below procedure. Approximately 2 mg of the quercetin-loaded EPS sample was suspended in phosphate buffer (pH 7.4). The size distribution of the quercetin-loaded EPS was determined via laser diffraction using a particle size analyzer at 25°C ± 1°C (Nano-ZS Zen 3600, Malvern Ltd., Malvern, UK). Particle size measurements were performed at a scattering angle of detection of 90°C, and the average

particle size measurements were performed in triplicate. The sample was then subjected to laser Doppler anemometry and photon correlation spectroscopy using the Zetasizer (Nano-ZS Zen 3600, Malvern Ltd., Malvern, UK) instrument equipped with a He-Ne laser operating with a scattering detector. Approximately, 2 mg of quercetin-loaded EPS was added to the vial, and the zeta potential was measured in fresh phosphate-buffered saline (pH 7.4) at 25°C. All measurements were performed in triplicate.

Surface characterization and composition analysis

Furthermore, surface characteristics were studied using scanning electron microscopy (SEM) and elemental analysis was performed using energy dispersive X-ray analysis (EDAX) linked to SEM (Bruker, Germany, Model Nano X Flash Detector). The thermal properties of quercetin-loaded EPS were studied using thermogravimetric analysis (TGA). A thermal analyzer operating over a range of 30 to 800°C at 20°C/min (NETZSCH STA 449F3 STA449F3A-1100-M) was used to study the changes in mass with respect to changes in temperature in an inert N_2 environment.

Estimation of quercetin

The aluminum chloride colorimetric method was used for the determination of quercetin in quercetin-loaded EPS. The fundamental idea behind the colorimetric technique using aluminum chloride is that aluminum chloride reacts with the C-4 keto group and either the C-3 or C-5 hydroxyl group of flavones and flavonols to generate acid-stable complexes, which give rise to a yellowish to orange colour that can be detected at 510 nm using a UV-visible spectrophotometer[6]. A standard calibration curve was constructed. Briefly, a quercetin stock solution was prepared by dissolving 1 g of quercetin in 100 mL of methanol (10 mg/mL). Quercetin working standards were prepared in the range of 0.1 mg/mL to 5 mg/mL. 100µL of each dilution was mixed with 500 µL of distilled water and 100 µL of 5% sodium nitrate solution and allowed to stand for 6 min. Approximately 150 µL of 10% aluminum chloride solution was added to the mixture, and the sample was incubated for 5 min, followed by the addition of 200 µL of 1M sodium hydroxide solution. Then, the absorbance of the sample was measured spectrophotometrically at 510 nm[7]. All measurements were performed in triplicate.

Loading efficiency and loading capacity

1 mL of the drug-loaded EPS solution was mixed with 49 mL of phosphate buffer at pH 7.4[8]. The amount of free quercetin present in the buffer was measured using UV-visible spectrophotometer at 510 nm, as discussed in the estimation of quercetin. All measurements were performed in triplicate. The loading efficiency (LE) and loading capacity (LC) of the EPS were calculated according to the following equations.

$$\text{Loading efficiency (\%)} = \frac{(\text{initial weight of quercetin} - \text{weight of free quercetin})}{\text{initial weight of quercetin}} \times 100 \quad \ldots(1)$$

$$\text{Loading capacity} = \frac{(\text{initial weight of quercetin} - \text{weight of free quercetin})}{\text{weight of quercetin-loaded EPS}} \quad \ldots(2)$$

***In vitro* drug release study**

Briefly, 2 mL of quercetin-loaded EPS solution was transferred into a dialysis bag (2 KDa cut-off), which was immersed in 100 mL of PBS (pH 7.4) and incubated at 37°C at 100 rpm. All drug-release media were withdrawn after certain intervals and restored with an equal volume of fresh medium[9]. The amount of quercetin released into the buffer solution was measured using UV-visible spectrophotometer at 510 nm by a flavonoid assay as described in the estimation of quercetin. The percentage drug release (%) of the quercetin-loaded EPS was calculated according to the following equation:

$$\text{Percentage drug release}(\%) = \frac{(A_0 - A_1) * 100}{A_0} \quad \ldots(3)$$

where A_0 is defined as the absorbance of the control and A_1 is defined as the absorbance of the sample[10].

The cumulative drug release (%) of the quercetin-loaded EPS was calculated according to the following equation:

$$\text{Cumulative drug release}(\%) = \frac{\text{volume of sample withdrawn}}{\text{total volume}} * P_{(t-1)} + P_t \quad \ldots(4)$$

where P_t is the amount of drug released at time t and $P_{(t-1)}$ is the amount of drug released prior to time t[11,12].

Kinetic analysis of the drug release profile

The *in vitro* drug release kinetics data were computed using DD solver 1.0 software, and the data were statistically analyzed by fitting to various mathematical models, such as zero-order (cumulative percentage drug release vs. time), first-order (log percentage drug remaining vs. time), Korsmeyer-

Peppas (log drug release vs. log time), and Peppas-Sahlin (cumulative percentage drug release vs. time) models, to verify the kinetics of drug release[13]. The kinetic equations that were used to study the drug release mechanism are mentioned below:

Zero-order kinetics, $Q = Q_0 + K_0 t$ … (5)

First-order kinetics, $\text{Log } C_t = \text{Log } C_0 - Kt / 2.303$… (6)

Peppas Shalin model, $M_t/M_\infty = k_1 t^n + k_2 t^{2n}$ … (7)

Korsmeyer-peppas model, $M_t / M_\alpha = Kt^n$ … (8)

Where Q is the amount of drug released, Q_0 is the initial amount of the drug, K_0 is the constant of zero-order release, C_0 is the initial drug concentration, C_t is the concentration of the drug in the solution at time t, K is the first-order rate constant ($time^{-1}$), M_t/M_∞ is the fraction of drug released at time t, k is the constant of the release kinetics, n is the exponent indicative of the mechanism of release and the release exponent that represents the drug's method of transport for the Peppas-Shalin model and the Korsmeyer-Peppas model, respectively.

Stability studies

Equal volumes of 10% sodium chloride (NaCl) (w/v), 0.5% pepsin, trypsin, and alpha-amylase (w/v), and 0.01 M phosphate buffer solutions (pH 3.2, 5.4, and 7.4) were added to the freshly prepared EPS-based quercetin-loaded microparticle suspension (1 mL) separately and maintained at 37 ± 1°C for 48 h. The phosphate buffer solutions of pH 3.2, 5.4, and 7.4 were selected to represent acidic, slightly acidic, and physiological environments relevant to drug release studies. pH 3.2 simulates gastric conditions, pH 5.4 represents slightly acidic microenvironments such as inflamed or tumor tissues, and pH 7.4 corresponds to physiological blood and tissue pH[14]. After 48 h of incubation, the absorbance of each quercetin-loaded EPS suspension was measured[9].

Functional characterization of quercetin-loaded EPS

Antioxidant activity

DPPH radical scavenging activity was determined by adding 2 mL of 0.1 mmol/L of α, α-diphenyl-β-picrylhydrazyl (DPPH) (in 100% ethanol) to 2 mL of quercetin, EPS, and quercetin-loaded EPS, respectively. The mixture was incubated for approximately 30 min in the dark at room temperature. The absorbance of the solutions was measured at 517 nm[15]. All measurements were performed in triplicate (n = 3). The mean and standard deviation (SD) were calculated using Microsoft Excel 365. The DPPH radical-scavenging antioxidant potential (%) was calculated using Eq. (9),

$$\text{Antioxidant potential (\%)} = 1 - \frac{A_s - A_c}{A_0} * 100 \ldots(9)$$

Where A_s, A_c, and A_0 denote the absorbance values of the sample, control (in which the DPPH solution was replaced with ethanol), and blank (in which the sample was replaced with ethanol).

Anti-inflammatory activity

The anti-inflammatory activities of quercetin, EPS, and quercetin-loaded EPS were determined. The samples used for this assay include 0.2 mL of egg albumin (fresh), 2.8 mL of phosphate-buffered saline (PBS, pH 6.4), and 2 mL of quercetin, EPS, and quercetin-loaded EPS, respectively, reconstituted with 2% Tween 80 dissolved in double-distilled water. The samples were mixed slowly and incubated at 37 °C for 15 min, followed by incubation in a water bath at 70°C for 5 min. The sample was then cooled to room temperature, and the absorbance was measured at 660 nm spectrophotometrically[16]. Measurements were performed in triplicate (n = 3), and mean ± SD values were calculated in Microsoft Excel 365. The anti-inflammatory activity was measured by calculating the percentage inhibition of protein denaturation, which was estimated by considering denaturation in control as 100% and calculated as follows:

$$\text{Percentage inhibition (\%)} = \frac{A_t}{A_c - 1} * 100 \quad \ldots(10)$$

Where, A_t is the absorbance of the test sample and A_c is the absorbance of the control (double-distilled water was used as the control).

Results and Discussion

Production and extraction of EPS

EPS was produced by *Bacillus* sp. EPS003 in the late log phase of bacterial growth as described in our previous publication[4] and extracted using the ethanol precipitation method. The precipitate obtained was freeze-dried. The previously reported carbohydrate and protein contents of EPS003 confirm the purity of the extracted product.

Characterization of quercetin-loaded EPS

The solution was initially light yellow after quercetin was added, but after constant stirring, it began to turn very clear. Self-assembled microparticles were indicated by the stirring mixture's formation of a stable colloidal suspension, which was further verified by UV-visible spectra. For

the quercetin-loaded EPS microparticles to be successfully synthesized, a thorough characterization employing a variety of analytical methods, such as spectroscopic, thermal, and morphological analyses, were essential. The findings of these analyses not only confirmed successful quercetin and drug conjugation but also offered crucial information regarding the chemical and physical interactions between the drug and the EPS carrier.

These results are fundamental because they validate the stability and structural integrity of the complex, both of which are necessary for its intended use as a controlled drug-delivery system.

UV–visible spectroscopy

Wavelength scans of quercetin, EPS, and quercetin-loaded EPS were performed in the range of 200-500 nm and the spectra are given in Fig. 1. EPS exhibited a maximum absorption at 230 nm, while quercetin showed two characteristic maxima at 370 nm and 410 nm; the 370 nm corresponds to the typical Band I transition of quercetin[17], whereas a secondary absorption around 410 nm was observed due to solvent effects as quercetin was dissolved in DMSO, which acted as the reference blank. Similar bathochromic shifts and shoulder bands above 400 nm have been reported for quercetin in solvents with strong solubilizing capacity, where solvent–solute interactions alter the electronic transitions of the cinnamoyl system[18]. Our observation is consistent with recent studies that have experimentally and theoretically confirmed a secondary absorption feature for quercetin in the 400–420 nm range in DMSO-containing solvent systems[19,20]. Quercetin-loaded EPS exhibited a new absorption feature near 250 nm, confirming the conjugation of quercetin with EPS. This observed shift in the absorption spectra confirms that quercetin is not merely a mixture with EPS but has formed a stable complex, a crucial step for developing an effective drug-delivery system.

Fourier transform infrared spectroscopy (FTIR)

Fig. 2 shows the FTIR spectra of quercetin, EPS, and quercetin-loaded EPS. Quercetin showed distinctive peaks for phenolic O-H and C=O stretching vibrations at 3410.15 cm^{-1} and 1658.78 cm^{-1}, respectively. Peaks connected to aromatic C=C and benzene ring stretching vibrations at 1527.62 cm^{-1}, C-O stretching vibrations associated with the ring stretch of the phenyl ring at 1265.30 cm^{-1}, and C-O-C symmetrical stretching at 1165 cm^{-1} were also

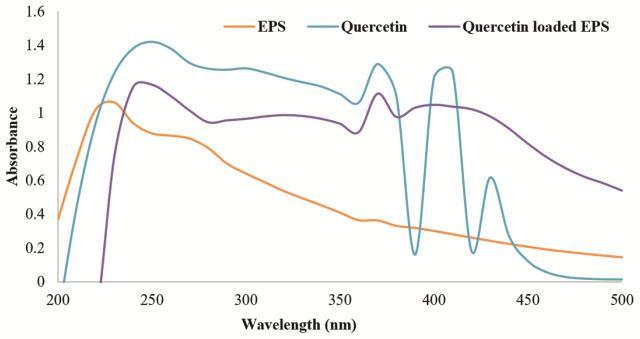

Fig. 1 — UV–visible absorption spectra of quercetin, EPS, and quercetin-loaded EPS microparticles

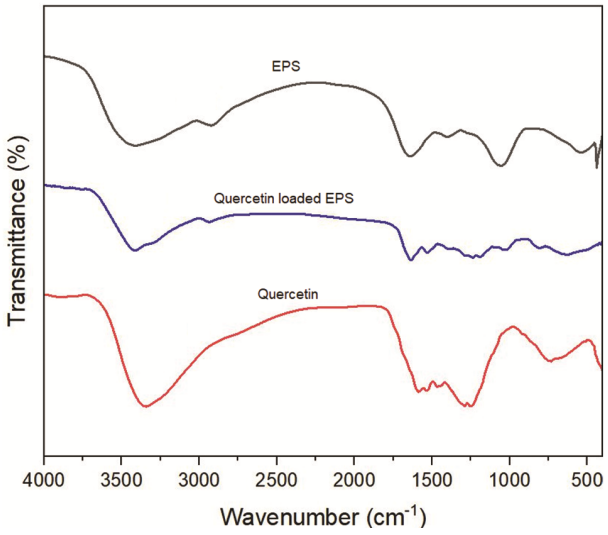

Fig. 2 — FTIR spectra of pure EPS, pure quercetin, and quercetin-loaded EPS microparticles

detected[21]. The bands at 941.26, 864.11, 825.53, 640.37, and 570.93 cm^{-1} were attributed to the bending vibrations of the C-H bonds, which are typical in organic compounds.

FTIR spectra of EPS showed a peak at 3394.72 cm^{-1} due to the presence of O-H groups. The observation of a characteristic peak at approximately 925.83 cm^{-1} is attributed to the stretching of glycosidic linkages between the fructose monomers in the EPS. Peaks observed at 1635.64, 1411.89, 1064.71, and 524.64 cm^{-1} correspond to H-O-H, stretching and bending vibrations of the C-H group, C-O stretching vibration, and the presence of fructose forms of sugar residues.

Upon loading quercetin onto the EPS, the FTIR spectrum of the quercetin-loaded EPS exhibited significant changes, indicating successful loading and interaction between the drug and the carrier. The successful loading of quercetin to EPS was confirmed by the formation of peaks at approximately

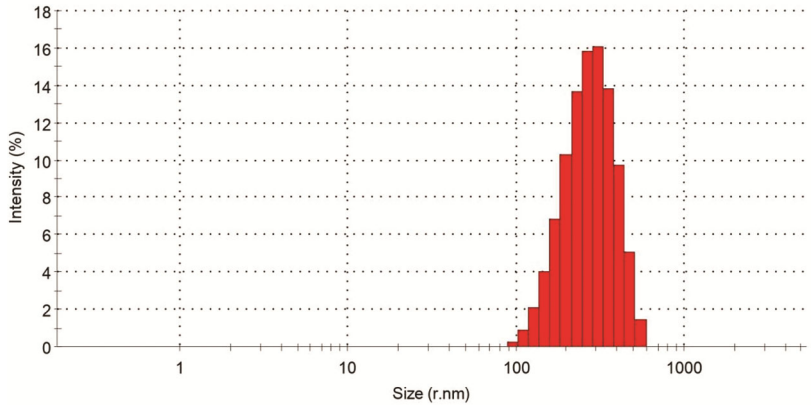

Fig. 3 — Particle size distribution of quercetin-loaded EPS microparticles obtained by dynamic light scattering

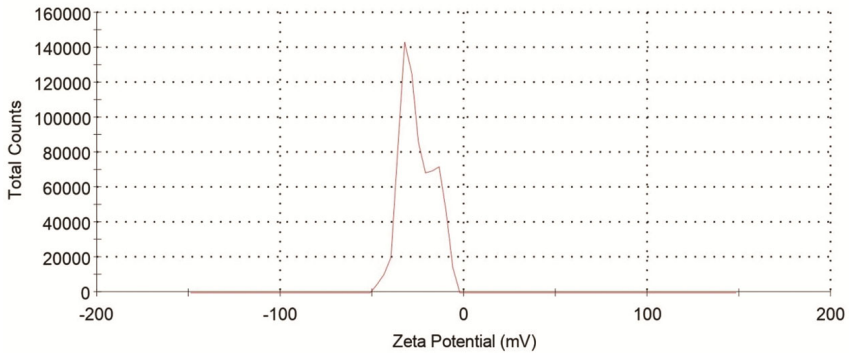

Fig. 4 — Zeta potential measurement of quercetin-loaded EPS microparticles showing surface charge and stability

3373-3422 cm^{-1} and 2918.2-2954 $cm^{-1,}$ which are attributed to H and OH interactions, suggesting the involvement of hydroxyl groups in the formation of a complex between quercetin and the EPS. This shift and broadening are indicative of hydrogen bonding interactions between the hydroxyl groups of quercetin and the polysaccharide backbone of the EPS. This is a crucial finding, as hydrogen bonding is a primary mechanism for the stable incorporation of polyphenolic compounds like quercetin into polysaccharide matrices.

Furthermore, the functional group interactions were were confirmed by the appearance of peaks at 1215 cm^{-1} and 1026 cm^{-1}, which are attributed to C-O stretching vibrations.These spectral shifts demonstrate that quercetin is more than just mixed with EPS; it has formed a stable conjugate, which is required for its function as a controlled-release drug-delivery system.

Analysis of particle size and zeta potential

From the dynamic light scattering analysis (Fig. 3), the particle size and zeta potential of quercetin-loaded EPS (Fig. 4) were found to be 710.94 nm and -25.4 mV, respectively. As per the literature, the above-mentioned values are suitable for use in drug-delivery applications. A high zeta potential promotes particle stability through electrostatic interactions, as repulsive forces prevent the MPs from aggregating with each other[22]. The negative charge obtained may be due to the presence of a hydroxyl and carboxylic groups contributed by quercetin and EPS in the conjugate formed by the EPS and quercetin interaction.

Scanning electron microscopy studies

Morphological analysis by SEM revealed that quercetin exhibited sharp and needle-like shapes as reported by Park *et al.*[23]. While a sheet-like compact morphology was observed for levan-type EPS[24]. Based on our previous observations reported, compact, amorphous, nonuniform blocks with microporous properties composed the matrix created by EPS[4]. SEM images of the quercetin-loaded EPS at various magnifications revealed that the EPS contributes to a glossy surface with a porous structure[25], while quercetin and EPS both contribute to irregular lumps of particles with branched morphologies to form microparticles of drug conjugated carriers, as shown in Fig. 5.

Compositional analysis using EDAX

EDAX analysis was performed to characterize the chemical composition and confirm the interaction of the

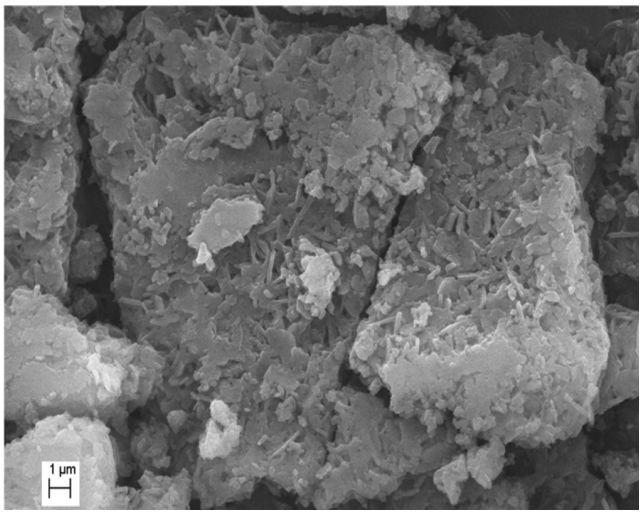

Fig. 5 — SEM images illustrating surface morphology of quercetin-loaded EPS microparticles

compounds of interest. Elemental analysis of the quercetin-loaded EPS revealed the predominant presence of carbon (52.3%) and oxygen (34.4%), which are characteristics of both EPS and quercetin along with the presence of other elements in small amounts, as shown in Fig. 6. These additional peaks may be attributed to interactions between quercetin functional groups and the polysaccharide backbone, thereby indicating successful quercetin loading.

Thermogravimetric analysis

The thermal stability of quercetin-loaded EPS was analyzed using thermogravimetric analysis (TGA) as stability is a crucial factor that influences the stability of polymer-drug conjugates in drug-delivery applications, and the results are shown in Fig. 7.

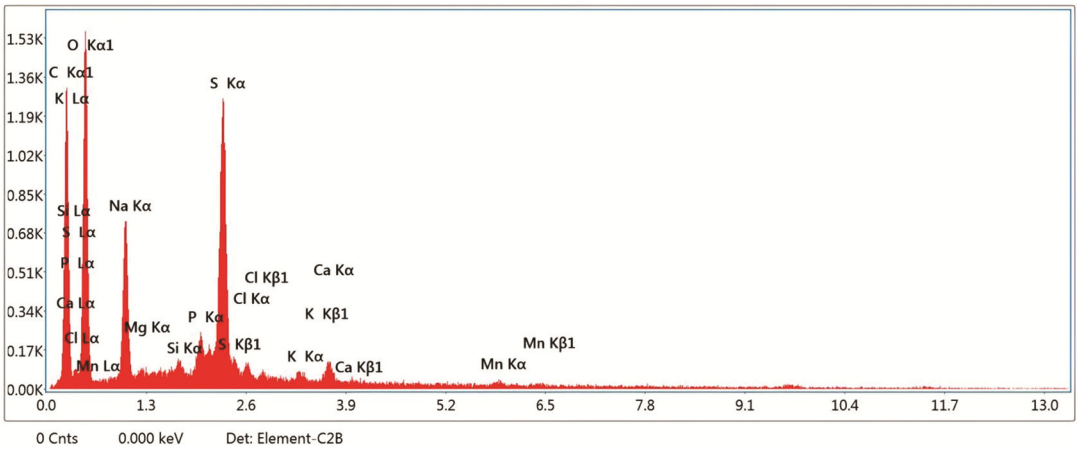

Fig. 6 — EDAX spectrum of quercetin-loaded EPS microparticles

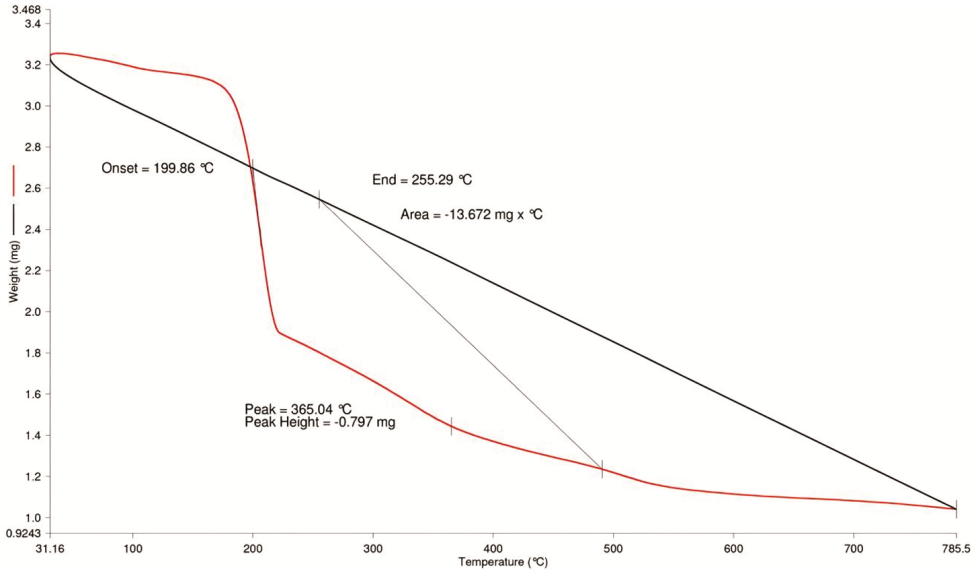

Fig.7 — TGA thermogram of quercetin-loaded EPS microparticles

TGA is a standard technique in drug-delivery for characterizing the thermal behaviour of the new formulations. In this study it was used to confirm the formation of the complex and to assess its thermal stability, which is a key parameter in determining appropriate formulation, storage, and handling conditions[26].

TGA profiles of pure quercetin[27] and EPS[4,28] have already been extensively reported in the literature; hence, only the conjugate was analyzed in this study. The quercetin-loaded EPS was thermally stable in the range of 0–180°C, with no sharp decrease in weight observed. A sudden decrease in weight of 34–39% in the range of 180–205°C could be attributed to the loss or evaporation of water molecules that were strongly bound within the complex. This serves as supporting evidence for the interaction between quercetin and the EPS matrix since this event occurred at a considerably higher temperature than typical moisture evaporation. Above 200°C, a significant decrease in the weight to 64% of the original weight could be observed until 800°C. This period refers to the degradation stage, which could be due to the gradual rupture of EPS branch linkages, the breaking of EPS chains, or disruption of the pyranose ring structure[29].

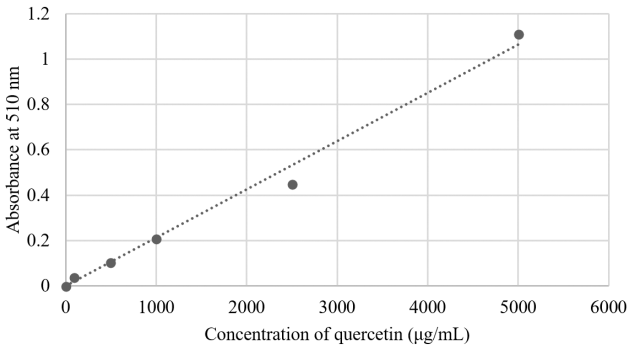

Fig. 8 — Standard curve for quercetin estimation

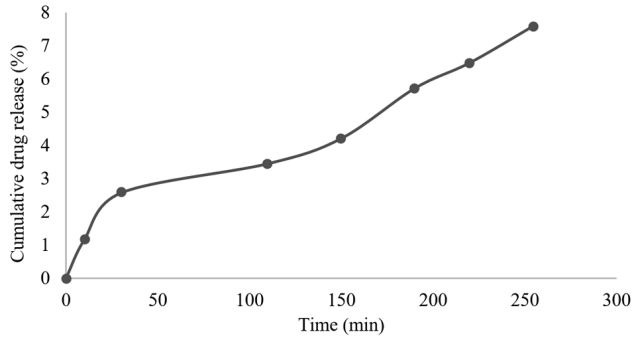

Fig. 9 — Drug release profile of quercetin

Andrew and Gurunathan[28] indicated that the breakdown temperature of levan EPS is roughly 225°C due to the polymer's strong thermal stability, but Bostan *et al*.[27] noted that the decomposition range of quercetin lies between 428 and 605°C. The broader and altered decomposition pattern of the quercetin-loaded EPS spanning 200-800°C suggests a physical or chemical interaction between the two components. These changes, compared to the individual components, confirm that the complex retains thermal stability within a physiologically relevant range, supporting its potential utility in drug-delivery formulations.

Estimation of quercetin

A standard curve was plotted between the concentration of quercetin and the absorbance at 510 nm, as shown in Fig. 8. The standard graph was used to estimate quercetin in all other experiments.

Loading efficiency and loading capacity

The loading efficiency and capacity of EPS calculated using Eqs (1) and (2) are found to be 96.25% and 48%, respectively. Higher loading efficiency and loading capacity may be due to the interaction of functional groups and the surface properties of quercetin and EPS. These values are at the high end of what is typically reported for polysaccharide-based carriers. When compared with established polysaccharide carriers, EPS003 exhibits distinct advantages. Similar bacterial EPS such as levan and kefiran have been explored as drug carriers but generally show lower drug loading (50–80%) and limited enzymatic stability[30,31]. In contrast, EPS003 microparticles achieved 96.25% and exhibited robust resistance to enzymatic degradation, underscoring their novelty and potential in drug-delivery.

In vitro quercetin release from quercetin-loaded EPS

The quercetin release profiles from quercetin-loaded EPS in phosphate buffer at pH 7.4 are shown in Fig. 9. The release profile is plotted as a cumulative percentage of drug release versus time and shows that the amount of quercetin released from the quercetin-loaded EPS gradually increased with time.

For *in vitro* drug release kinetic analysis of the quercetin-loaded EPS, various models, such as the zero-order kinetic model (Fig. 10a), the first-order kinetics model (Fig. 10b), the Korsmeyer-Peppas model (Fig. 10c), and the Peppas-Shalin model (Fig. 10d), were fitted.

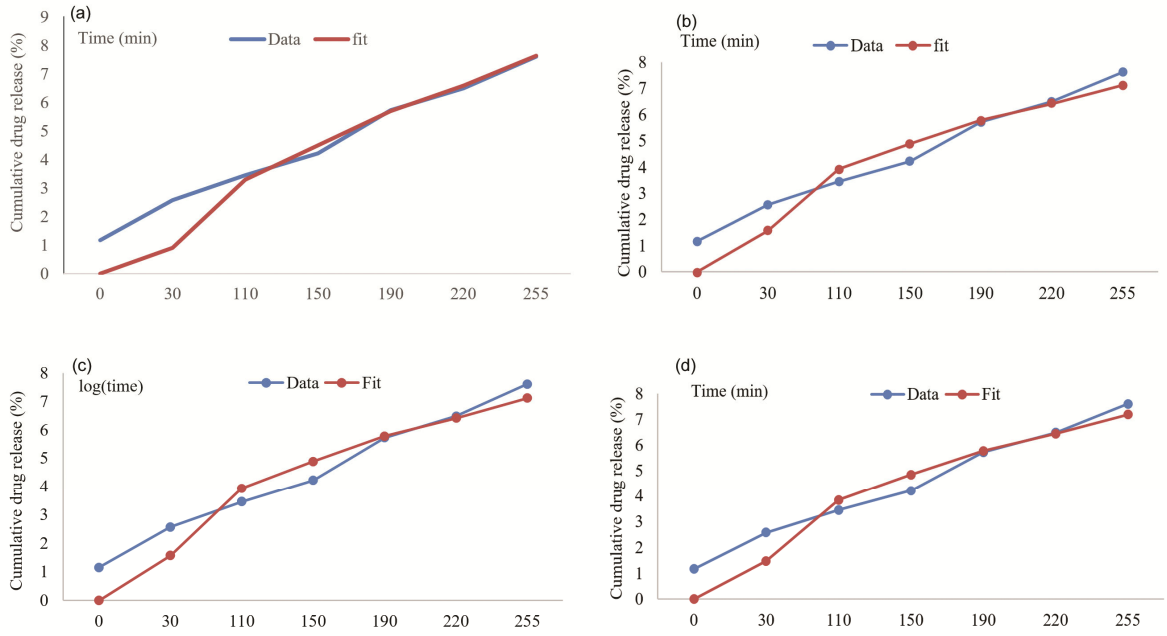

Fig. 10 — Drug release kinetics plots fitted to (a) zero-order kinetics, (b) first order kinetics, (c) Korsmeyer–Peppas and (d) Peppas–Sahlin model

Table 1 — Quercetin release kinetics

Model	r^2	K	n	SSO
Zero order $F = K_0 \times t$	0.9839	0.02995	-	4.2548
First order $F = 100 \times [1-\exp(-K_1 \times t)]$	0.9680	0.0914	0.3989	0.0162
Korsmeyer-Peppas model $F = k_{KP} \times t^n$	0.9645	0.1406	0.6091	3.2950
Peppas-Sahlin model $M_t/M_\infty = k_1 t^n + k_2 t^{2n}$	0.9713	0.1220	0.7081	3.2719

The kinetic profiles of each of these models are depicted in Table 1; where r^2 = Correlation coefficient, K = Kinetics constant, n = Diffusion coefficient, SSO = Sum of square order, F = the fraction of drug released at time t, K_0 = the zero-order release rate constant, k_1 = the first-order release constant, k_2 = the second-order release constant, k_{KP} = the Korsmeyer–Peppas rate constant, M_t/M_∞ = the fraction of drug released at time t, k = the kinetics constant, n = the diffusion constant, r^2= the squared correlation coefficient, and SSO = the sum of squares of the order. icles. Data expressed as mean ± SD (n = 3)

For each model, the kinetic release constant (k) and the correlation coefficient (r^2) were determined and tabulated in Table 1. The r^2 value of the zero-order kinetics model was greater than that of the first-order kinetics model. The release profile was gradual and sustained at pH 7.4, with the zero-order kinetics providing one of the best fits ($r^2 \approx 0.98$), consistent with Fickian diffusion-controlled release from hydrated polysaccharide matrices. Diffusion-dominated release has been likewise reported for several microbial and plant-derived polysaccharide systems, including dextran and pullulan carriers[32,33] formulated as micelles, nanoparticles, hydrogels, or spray-dried microparticles for mucosal/oral delivery[34]. The consistency of EPS003 with this release pattern, while achieving high loading efficiency, highlights its potential as a robust natural EPS carrier for sustained therapeutic delivery.

Stability studies

The maximum absorbance of quercetin-loaded EPS samples in phosphate buffers of different pH 3.2, 5.4, and 7.4, 10% NaCl, and 0.5% enzymatic solutions (alpha-amylase, pepsin, and trypsin) was found to be approximately 250 nm (Fig. 11). This result indicates the stability of the quercetin-loaded EPS sample at various pH values and in different media. In addition, none of the enzymatic solutions showed signs of enzymatic breakdown. The stability of the quercetin-loaded EPS microparticles across this pH range (3.2–7.4) indicates their robustness under physiologically relevant acidic to neutral environments, suggesting suitability for oral delivery and systemic stability. Many polysaccharide carriers (including some dextran/pullulan derivatives) become susceptible to hydrolysis or enzyme-mediated erosion depending on linkage chemistry and substitution; the

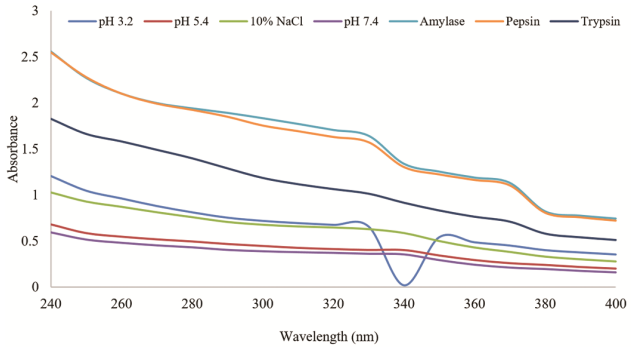

Fig. 11 — Stability of quercetin-loaded EPS microparticles in buffers (pH 3.2, 5.4, 7.4), 10% NaCl, and enzymes (α-amylase, pepsin, trypsin)

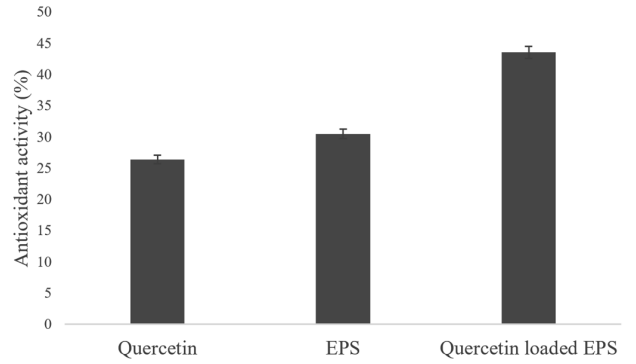

Fig. 12 — Antioxidant activity (DPPH radical scavenging assay) of pure quercetin, EPS and quercetin-loaded EPS microparticles [Data expressed as mean ± SD (n = 3)]

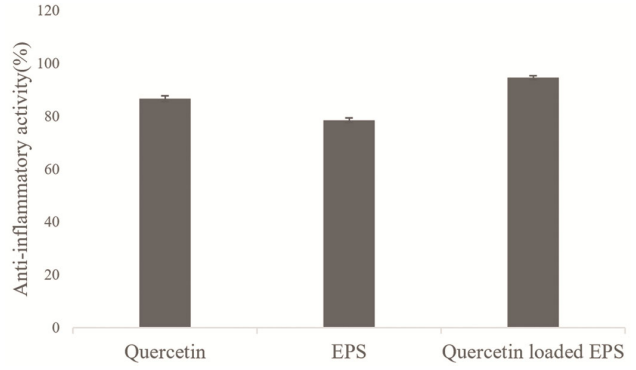

Fig. 13 — Anti-inflammatory activity (protein denaturation inhibition assay) of pure quercetin, EPS, and quercetin-loaded EPS microparticles

observed stability here indicates a matrix that is able to maintain integrity during gastrointestinal transit, which looks promising for oral delivery and for protecting hydrophobic flavonoids like quercetin prior to absorption. Recent reviews on microbial EPS emphasize precisely these desirable traits—biocompatibility, tunable chemistry, and the capacity to regulate and sustain release[35,36].

Antioxidant characteristics of quercetin-loaded EPS

Fig. 12 shows the free radical scavenging effect of quercetin, EPS, and quercetin-loaded EPS. The observed results indicate that the antioxidant potentials of quercetin, EPS, and quercetin-EPS were 26.40 ± 0.70%, 30.50 ± 0.78%, and 43.56 ± 0.96%, respectively. The antioxidant activity of quercetin-loaded EPS to scavenge DPPH radicals is found to be relatively higher than that of quercetin and EPS. Error bars in Fig. 12 represent mean ± SD. The assessment of antioxidant activity was important to confirm that drug loading to EPS enhanced the free radical scavenging efficiency of quercetin, supporting its potential role in mitigating oxidative stress–related damage[37]. Beyond quercetin's intrinsic activity, several bacterial EPS (LAB-EPS, levan, and dextran) possess modest radical-scavenging capacity; co-localization in the matrix can yield additive or synergistic effects reported across microbial EPS systems[38]. Since our work aims at exploring EPS as a delivery system, assessing antioxidant activity was also necessary to establish whether quercetin retains or enhances its functional characteristics post-encapsulation.

Anti-inflammatory property of quercetin-loaded EPS

The anti-inflammatory activity of quercetin, EPS, and quercetin-loaded EPS was assessed using the egg albumin denaturation assay. The results revealed a percentage inhibition of 86.70 ± 1.04% for quercetin, 78.50 ± 0.92% for EPS, and 94.60 ± 0.78% for quercetin-loaded EPS (Fig. 13).

Based on these findings, the EPS loaded with quercetin shows a notable anti-inflammatory effect in the egg albumin denaturation test. Furthermore, the anti-inflammatory activity of quercetin-loaded EPS is relatively higher than that of the drug and EPS. Error bars in Fig. 13 represent mean ± SD. Evaluation of anti-inflammatory activity was included to demonstrate that quercetin-loaded EPS provides greater protection against protein denaturation, highlighting its relevance in controlling inflammation-associated pathological processes[39]. Microbial EPS especially those from lactic acid bacteria are repeatedly linked to immunomodulatory/anti-inflammatory responses, providing a plausible supportive role of the carrier itself alongside the loaded quercetin[38]. Considering the potential application of EPS as a delivery vehicle, this assay also ensured that the loded quercetin preserves its anti-inflammatory efficacy.

The EPS003 matrix contributes intrinsic antioxidant and anti-inflammatory activity, suggesting multifunctionality where the carrier may work together with pharmacology of quercetin. Contemporary reviews of microbial EPS[40], particularly from lactic acid bacteria and other genera highlight their bioactive roles as antioxidant, anti-inflammatory, and immunomodulatory substances[41], motivating their use as functional excipients rather than passive vehicles. Our findings align with this trend and position EPS003 within the growing class of bioactive polysaccharide carriers.

Overall, EPS003 distinguishes itself among bacterial polysaccharide carriers by combining very high loading, diffusion-controlled sustained release, GI-relevant stability, thermal stabilization, and intrinsic bioactivity. In comparison to widely studied carriers such as dextran, pullulan, and levan, EPS003 delivers comparable or superior performance on critical metrics while offering the added advantage of endogenous bioactivity. These attributes support its potential for oral and mucosal delivery of polyphenols and other hydrophobic drugs and warrant further *in vivo* evaluation and scale-up studies.

Conclusion

In this research, a model drug, quercetin was loaded onto an exopolysaccharide using glutaraldehyde by the modified precipitation method. The loading efficiency and loading capacity of the synthesised conjugate were estimated to be 96.25% and 48%, respectively. Stability studies in various buffers and enzymatic solutions proved that the drug-loaded carrier is stable and can withstand adverse environmental changes. The sequential release of the drug in the phosphate buffer (pH 7.4) was successfully studied *in vitro*, which implies that the drug molecule is released from the drug carrier at regular intervals. It was then fitted into various models and found to follow zero-order kinetics and the Fickian mode of diffusion. The drug-loaded exopolysaccharide also exhibits biological activities like antioxidant activity and anti-inflammatory activity. A comparison between the *in vitro* and *in vivo* studies might provide insights on the possible changes that might be required for the drug-delivery carrier to be used for the treatment of cancer cells.

Acknowledgement

The authors wish to thank the management of Mepco Schlenk Engineering College for providing the necessary infrastructure to perform the above research.

Conflict of interest

The authors declare no conflict of interest.

References

1 Trucillo P, Drug carriers: Classification, administration, release profiles, and industrial approach, *Processes*, 9 (2021) 470.

2 Ezike T C, Okpala U S, Onoja U L, Nwike C P, Ezeako E C, Okpara O J, Okoroafor C C, Eze S C, Kalu O L, Odoh E C, Nwadike U G, Ogbodo J O, Umeh B U, Ossai E C & Nwanguma B C, Advances in drug-delivery systems, challenges and future directions, *Heliyon*, 9 (2023) e17488.

3 Kalimuthu A K, Pandian S R K, Pavadai P, Panneerselvam T, Kabilan S J, Sankaranarayanan M, Ala C & Kunjiappan S, Drug-delivery applications of exopolysaccharides from endophytic bacteria pseudomonas otitidis from tribulus terrestris L, *J Polym Environ*, 31 (2023) 3632.

4 Marimuthu S & Rajendran K, Structural and functional characterization of exopolysaccharide produced by a Novel Isolate Bacillus sp. EPS003, *Appl Biochem Biotechnol*, 195 (2023) 4583.

5 Marimuthu S, Pappu J S M P & Rajendran K Artificial neural network modeling and statistical optimization of medium components to enhance production of exopolysaccharide by Bacillus sp.EPS003, *Prep Biochem Biotechnol*, 53 (2022) 136.

6 Ahmed F & Iqbal M, Antioxidant activity of *Ricinus Communis*, *Org Med Chem Int J*, 5 (2018) 555667.

7 Shirazi O U, Khattak M M A K, Shukri N A M & Anuar M N N, Determination of total phenolic, flavonoid content and free radical scavenging activities of common herbs and spices, *J Pharmacogn Phytochem*, 3 (2014) 104.

8 Zou Y, Qian Y, Rong X, Cao K, McClements D J & Hu K, Encapsulation of quercetin in biopolymer-coated zein nanoparticles: Formation, stability, antioxidant capacity, and bioaccessibility, *Food Hydrocoll*, 120 (2021) 106980.

9 Vanavil B, Selvaraj K, Aanandhalakshmi R, Sri K U & Arumugam M, Bioactive and thermostable sulphated polysaccharide from Sargassum swartzii with drug-delivery applications, *Int J Biol Macromol*, 153 (2020) 190.

10 Kunjiappan S, Panneerselvam T, Somasundaram B, Arunachalam S, Sankaranarayanan M & Parasuraman P, Preparation of liposomes encapsulated Epirubicin-gold nanoparticles for Tumor specific delivery and release, *Biomed Phys Eng Exp*, 4 (2018) 045027.

11 Dash S, Murthy P N, Nath L & Chowdhury P, Kinetic modeling on drug release from controlled drug-delivery systems, *Acta Pol Pharm*, 67 (2010) 217.

12 Chandrasekaran A R, Jia C Y, Theng C S, Muniandy T, Muralidharan S & Dhanaraj S A, In vitro studies and evaluation of metformin marketed tablets-Malaysia, *J Appl Pharm Sci*, 1 (2011) 214.

13 Heredia N S, Vizuete K, Flores-Calero M, Pazmiño V K, Pilaquinga F, Kumar B & Debut A, Comparative statistical analysis of the release kinetics models for nanoprecipitated drug-delivery systems based on poly(lactic-co-glycolic acid), *PLoS One*, 17 (2022) e0264825.

14 Lazzari S, Moscatelli D, Codari F, Salmona M, Morbidelli M & Diomede L, Colloidal stability of polymeric nanoparticles in biological fluids, *J Nanopart Res*, 14 (2012) 920.

15 Yang D, Wang T, Long M & Li P, Quercetin: Its main pharmacological activity and potential application in clinical medicine, *Oxid Med Cell Longev*, 2020 (2020) 8825387.

16 Lee G H, Lee S J, Jeong S W, Hyun-Chul K, Park G Y, Lee S G & Choi J H, Antioxidative and antiinflammatory activities of quercetin-loaded silica nanoparticles, *Colloids Surf B*, 143 (2016) 511.

17 Srivastava N, Bansal A, Aggarwal K & Nagpal K, Development and validation of UV spectrophotometric method for the quantitative estimation of quercetin in bulk followed by its solubility studies, *J Appl Spectrosc*, 91 (2024) 700.

18 Buchweitz M, Kroon P A, Rich G T & Wilde P J, Quercetin solubilisation in bile salts: A comparison with sodium dodecyl sulphate, *Food Chem*, 211 (2016) 356.

19 Tamayo-Ramos J A, Martel S, Barros R, Bol A, Atilhan M & Aparicio S, On the behavior of quercetin+ organic solvent solutions and their role for C60 fullerene solubilisation, *J Mol Liq*, 345 (2021) 117714.

20 Abbot V & Sharma P, Thermodynamic and acoustic studies of quercetin with sodium dodecyl sulfate in hydro-ethanolic solvent systems: A flavonoid-surfactant interaction study, *Chem Phys*, 538 (2020) 110921.

21 Chellappan D K, Yee N J, Singh B J K A J, Panneerselvam J, Madheswaran T, Chellian J, Satija S, Mehta M, Gulati M, Gupta G & Dua K, Formulation and characterization of glibenclamide and quercetin-loaded chitosan nanogels targeting skin permeation, *Ther Deliv*, 10 (2019) 281.

22 Pochapski D J, dos Santos C C, Leite G W, Pulcinelli S H & Santilli C V, Zeta potential and colloidal stability predictions for inorganic nanoparticle dispersions: Effects of experimental conditions and electrokinetic models on the interpretation of results, *Langmuir*, 37 (2021) 13379.

23 Park S, Song I S & Choi M K, Preparation and characterization of quercetin-loaded solid dispersion by solvent evaporation and freeze-drying method, *Mass Spectrom Lett*, 7 (2016) 79.

24 Taylan O, Yilmaz M T & Dertli E, Partial characterization of a levan type exopolysaccharide (EPS) produced by Leuconostocmesenteroides showing immunostimulatory and antioxidant activities, *Int J Biol Macromol*, 136 (2019) 436.

25 Wang J, Xiao H, Zhao F, Zhao B, Xu M, Zhou Z & Han Y, A fructan sucrase secreted extracellular and purified in one-step by gram-positive enhancer matrix particles, *Processes*, 9 (2021) 95.

26 Agapakis G, Siamidi A, Kikionis S, Vlachou M & Pippa N, A thermal-analysis-technique-based mechanistic approach toward the release of omeprazole from solid dosage forms, *Sci Pharm*, 92 (2024) 8.

27 Bostan M S, Mutlu E C, Kazak H, Keskin S S, Oner E T & Eroglu M S, Comprehensive characterization of chitosan/PEO/levan ternary blend films, *Carbohydr Polym*, 102 (2014) 993.

28 Andrew M & Jayaraman G, Molecular characterization and biocompatibility of exopolysaccharide produced by moderately halophilic bacterium virgibacillus dokdonensis from the saltern of kumta coast, *Polymers*, 14 (2022) 3986.

29 da Costa E M, Filho J M B, do Nascimento T G & Macêdo R O, Thermal characterization of the quercetin and rutin flavonoids, *Thermochim Acta*, 392–393 (2002) 79.

30 Tan K, Chamundeswari V N & Loo S C J, Prospects of kefiran as a food-derived biopolymer for agri-food and biomedical applications, *RSC Adv*, 10 (2020) 25339.

31 Sezer A D, Kazak H, Öner E T & Akbuğa J, Levan-based nanocarrier system for peptide and protein drug-delivery: Optimization and influence of experimental parameters on the nanoparticle characteristics, *Carbohydr Polym*, 84 (2010) 358.

32 Petrovici A R, Pinteala M & Simionescu N, Dextran formulations as effective delivery systems of therapeutic agents, *Molecules*, 28 (2023) 1086.

33 Thakur A, Sharma S, Naman S & Baldi A, Pullulan based polymeric novel drug-delivery systems: A review on current state of art and prospects, *J Drug-Deliv Sci Technol*, 90 (2023) 105117.

34 Liu T, Gong X, Cai Y, Li H & Forbes B, Pullulan-based spray-dried mucoadhesive microparticles for sustained oromucosal drug-delivery, *Pharmaceutics*, 16 (2024) 460.

35 Nadzir M M, Nurhayati R W, Idris F N & Nguyen M H, Biomedical applications of bacterial exopolysaccharides: A review, *Polymers*, 13 (2021) 530.

36 Tabernero A & Cardea S, Microbial exopolysaccharides as drug carriers, *Polymers*, 12 (2020) 2142.

37 Forman H J & Zhang H, Targeting oxidative stress in disease: Promise and limitations of antioxidant therapy, *Nat Rev Drug Discov*, 20 (2021) 689.

38 Jurášková D, Ribeiro S C & Silva C C G, Exopolysaccharides produced by lactic acid bacteria: From biosynthesis to Health-Promoting properties, *Foods*, 11 (2022) 156.

39 Aghababaei F & Hadidi M, Recent advances in potential health benefits of quercetin, *Pharmaceuticals*, 16 (2023) 1020.

40 Liu W, Wei Y, Xiang R, Dong B & Yang X, Lactic acid bacteria exopolysaccharides unveiling multifaceted insights from structure to application in foods and health promotion, *Foods*, 14 (2025) 823.

41 Khalkhali M, Sadighian S, Rostamizadeh K, Khoeini F, Naghibi M, Bayat N, Habibizadeh M & Hamidi M, Synthesis and characterization of dextran coated magnetite nanoparticles for diagnostics and therapy, *Bioimpacts*, 5 (2015) 141.